Particulate matter and COVID-19 excess deaths: Decomposing long-term exposure and short-term effects

Leonardo Becchetti [a,*], Gabriele Beccari [a], Gianluigi Conzo [a], Pierluigi Conzo [b], Davide De Santis [c], Francesco Salustri [d]

[a] *University of Rome Tor Vergata, Department of Economics and Finance, Italy*
[b] *University of Turin, Department of Economics and Statistics "Cognetti de Martiis" & Collegio Carlo Alberto, Italy*
[c] *University of Rome Tor Vergata, Department of Civil Engineering and Computer Science Engineering, Italy*
[d] *University College London, Institute for Global Health, United Kingdom*

ARTICLE INFO

ABSTRACT

We investigate the time-varying effect of particulate matter (PM) on COVID-19 deaths in Italian municipalities. We find that the lagged moving averages of $PM_{2.5}$ and PM_{10} are significantly related to higher excess deceases during the first wave of the disease, after controlling, among other factors, for time-varying mobility, regional and municipality fixed effects, the nonlinear contagion trend, and lockdown effects. Our findings are confirmed after accounting for potential endogeneity, heterogeneous pandemic dynamics, and spatial correlation through pooled and fixed-effect instrumental variable estimates using municipal and provincial data. In addition, we decompose the overall PM effect and find that both pre-COVID long-term exposure and short-term variation during the pandemic matter. In terms of magnitude, we observe that a 1 $\mu g/m^3$ increase in $PM_{2.5}$ can lead to up to 20% more deaths in Italian municipalities, which is equivalent to a 5.9% increase in mortality rate.

1. Introduction

The impact of the COVID-19 pandemic in relation to contagion and deaths in the first half of 2020 is markedly heterogeneous from a geographical perspective. Several studies have tried to identify the causal factors of this puzzling outcome. Epidemiological literature has identified the frequency of human physical interactions as a leading causal factor of contagions. However, even after controlling for these factors, a significant part of the observed variability of COVID-19-related outcomes remains unexplained. This paper aims to shed light on this issue by investigating the role of particulate matter (PM) in the pandemic's high mortality rate.

The theoretical background for our research hypothesis can be summarized into two main literature strands. The first strand deems long-term exposure to PM as a contributing factor to COVID-19-related deaths. The research hypothesis relies on the maintained assumption that PM inhalation induces inflammation and oxidative stress, thereby reducing lung efficiency and contributing to respiratory and pulmonary diseases (see Pope and Dockery, 2006). Over the years, several empirical papers have estimated the relationship between long-term exposure to PM and total mortality, and mortality from cardiovascular and respiratory diseases (Kim et al., 2015; Pelucchi et al., 2009; Pinault et al., 2017; Faustini et al., 2011; Anderson, 2020; Ciencewicki and Jaspers, 2007; Sedlmaier et al., 2009) as well as the effect of fine PM as a factor in cardiovascular and respiratory morbidity and mortality (McGuinn et al., 2017; Jeong et al., 2017; Yin et al., 2017; Cakmak et al., 2018).

Based on this literature strand, several researchers have tried to

---

* Corresponding author at: Dept. of Economics and Finance, University of Rome Tor Vergata, via Columbia, 2, 00153 Rome, Italy.
  E-mail address: becchetti@economia.uniroma2.it (L. Becchetti).

ascertain if the effect of COVID-19 on respiratory and pulmonary diseases can be enhanced by PM exposure. Wu et al. (2020) found that an increase in exposure to $PM_{2.5}$ is associated with increased COVID-19 fatality in the US, Cole et al. (2020) find similar results for the Netherlands.[1] Focusing on Italy, Cartenì et al. (2020) find that the number of days in 2019 in which the national PM_{10} exceeded the 50 μg/m^3 daily limit is positively correlated with the number of certified daily cases. Perone (2020) finds that the case fatality rate is affected by ozone and nitrogen dioxide beyond PM, while Becchetti et al. (2022) used mortality data at province level to confirm this relationship controlling for several concurring factors. Coker et al. (2020) found support for the relationship in Northern Italy, estimating that a 1 μg/m^3 increase in $PM_{2.5}$ is associated with a 9% increase in COVID-19-related mortality. Many other studies have been conducted using different geographical samples to confirm the positive relationship between long-term exposure to PM and increase in COVID-19-related deaths (Ogen, 2020; Magazzino et al., 2020; Yongjian et al., 2020; Travaglio et al., 2021; Setti et al., 2020; Comunian et al., 2020).

The second strand of literature developed a theoretical hypothesis on the relevance of short term effects and on the role of PM as a carrier of the SARS-CoV-2 virus. Preliminary findings in this direction are found by Setti et al. (2020). The authors show the presence of SARS-CoV-2 viral RNA by detecting highly specific RtDR gene on eight filters in two parallel PCR analyses on 34 PM_{10} samples of outdoor/airborne PM_{10} in Bergamo province. However, they state that it is impossible to assess the viral charge of the carried virus outside the human body. Following this hypothesis, Delnevo et al. (2020) find that the lagged PM Granger causes adverse COVID-19 outcomes in several Italian provinces located in the Emilia-Romagna region. Similarly, Zoran et al. (2020) find a correlation between daily average ground levels of particulate matter concentrations and new cases and deaths in Milan. Isphording and Pestel (2020) conduct the same analysis for German regions. In the same vein, Austin et al. (2020) find that contemporary variation in PM significantly affects COVID-19 contagions and deaths in US counties, while Becchetti et al. (2020) use daily atmospheric data from the European regional level provided by the Copernicus Atmosphere Monitoring Service (CAMS) and find that $PM_{2.5}$ and PM_{10} concentration positively affects confirmed cases and deaths. They estimated that the effect peaks at the 6th to the 8th day lag for confirmed cases and the 13th day lag for deaths. In the opposite direction, Bontempi (2020) find, after assessing data from Lombardia and Piemonte, that it is impossible to conclude that COVID-19 diffusion also occurs through the air using PM_{10} as a carrier.

Our contribution is original with respect to the existing literature in several aspects. First, we disentangle the long-term exposure and the short-term effects to test the two aforementioned research hypotheses on the effect of PM on COVID-19 related outcomes in Italy simultaneously. Second, we control for heterogeneous pandemic dynamics and spatial correlation providing empirical evidence at both the municipality and province levels. Third, we control for the differential introduction of lockdown measures adopted by the Italian government. Fourth, we net out the effects of other unobservable time-invariant local confounders (i. e., municipal policies and regional health systems) at the finest and more disaggregated geographical level through municipality fixed effects. Last, we use instrumental variable approaches to mitigate endogeneity concerns.

Our empirical findings show a positive and significant relationship

between particulate matter and excess deaths in Italian municipalities and provinces during the first pandemic wave. Our results are robust and confirmed when using instrumental variables and when controlling for heterogeneous epidemics dynamics and spatial correlation. In terms of economic significance, we find that if conclusions from our IV estimates pointing at causality hold, a 1 μg/m^3 increase in $PM_{2.5}$ causes a 10–20% surge in excess deaths in Italian municipalities, depending on the model used. This is equivalent to an overall 3–6% increase in mortality rate.

2. Data

Our first data source is the Italian National Statistical Institute (ISTAT), which provides information on daily deaths in each municipality. We use the difference between daily deaths during the pandemic and the 2015–2019 five-year average of the corresponding days as the dependent variable (see Table A1 in the Appendix). This measure overcomes two well-known problems that arise when using official COVID-19 registered deaths. First, it is not always possible to ascertain whether victims died *because of* COVID-19 or *with* COVID-19, with Italy's independent local health systems, different municipalities, and regions that interpret this distinction differently. The resulting heterogeneity in death registration, therefore, creates an implicit measurement error. Second, at the peak of the pandemic in Italy—March and April 2020—hospitals were overcrowded and several COVID-19 victims could not access hospital care and died without a proper diagnosis.

The second and third data sources are the Copernicus Atmospheric Monitoring Service (CAMS) and the Copernicus Climate Change Service (C3S), which provide data on air quality data and weather conditions.[2] The analysis conducted in this paper exploits the following C3S datasets: (i) the C3S ERA5-Land hourly data from 1981 to present, which contains measures on various land variables over several decades at a global scale[3]; (ii) the CAMS European Air Quality Forecast, which provides information on air quality in Europe.[4]

We use the following variables:

- [C3S – ERA5-Land] 2 m temperature [K]: Air temperature at 2 m (height) obtained by interpolating the lowest model level and the Earth's surface; we converted temperature values to Celsius degrees by subtracting 273.15.
- [C3S – ERA5-Land] Total precipitation [m]: Accumulated precipitation in millimeters, including rain and snow, that falls to the

---

[1] By collecting data up to April 22, 2020, Wu et al. (2020) showed that an increase of $PM_{2.5}$ by 1 μg/m^3 is associated with an 8% increase in the COVID-19 death rate. Similarly, Cole et al. (2020) estimated the same relationship using data from 355 municipalities in the Netherlands. Their results provide evidence that an increase in $PM_{2.5}$ concentrations by 1 μg/m^3 is associated with an increase in COVID-19 deaths by 2.2 to 3%. In addition, they show that the same increase leads to a 9.4 to 15.1% rise in COVID-19 cases, and between 2.9 and 4.4% in COVID-19 hospital admissions.

[2] The Copernicus European program is one of the leading programs taking into account the environmental and terrestrial ecosystem monitoring, and it is becoming a widely used tool for measuring economic developments. It provides daily earth's information at different spatial resolution, varying from global to regional and even local scale, on a full, free, and open data policy. More information about the Copernicus program is available at https://www.coperni cus.eu/en.

[3] The dataset combines model *outputs* with observation across the world by means of physics laws, providing an accurate description of the current and past climate starting from January 1981 to the present. Data distribution is on hourly basis using a fixed square grid with 0.1 degrees of spatial resolution. The dataset has a monthly update frequency with a delay of about three months.

[4] The CAMS European air quality forecasts dataset allows for evaluating air pollution levels on a daily basis with a remarkable spatial resolution of 0.1 degrees in both latitude and longitude (approximately 10 km). Data production is based on nine air quality forecasting systems across Europe and a median ensemble calculated from their individual outputs, the combinations of these nine results provide a better performance than the individual model products on average. Model data are combined with observations provided by the European Environment Agency (EEA) into an integrated dataset using appropriate data assimilation techniques. The analysis is available at seven height levels at hourly time. We use ensemble method-based data, since this approach is useful and relevant for air quality analysis starting from a sample of individual model members (Galmarini et al., 2004).

Earth's surface considering possible steps during a single day; we converted precipitation values to millimeters by dividing by 1000.

- [CAMS – European Air Quality] Surface (average individual's height level) particulate matter d $<$ 2.5 μm [μg/m^3]: Fine solid or liquid particles in the atmosphere emitted by natural and anthropogenic sources with a diameter less than 2.5 μm (PM$_{2.5}$);
- [CAMS – European Air Quality] Surface (average individual's height level) particulate matter d $<$ 10 μm [μg/m^3]: Fine solid or liquid particles in the atmosphere emitted by natural and anthropogenic sources with a diameter less than 10 μm (PM$_{10}$).

The grid cover consists of points where the information is recorded spanning 0.1 degrees in latitude and longitude, i.e., the grid was made by the four points of the vertices. We use the Python-3 high-level programming language to download and process Copernicus data to extract the final dataset at the municipal level. Moreover, hour-specific filters were applied to get daily mean values averaging data available at 4-step hours during the day (8:00, 12:00, 20:00, 00:00) for the variables taken into account.

We identify the municipal polygon's centroid for each municipal area and define each municipal through its centroid. Since both weather and pollution variables are available according to a regular 10-km square grid, each centroid is associated with a variable's value based on minimum distance. By using this procedure, we obtain an average mean distance of less than 4 km. In many cases, the distance between the centroid and the closest grid is less than 1 km, which represents a sharp characterization of the real observations in the proximity of the spatial coordinates. In the section that follows, we explain how we use inverse distance weights to account for these differences.

Fig. 1 A–C provide clear descriptive evidence of the geographical distribution of PM$_{2.5}$ and PM$_{10}$ concentrations in relation to the geographical distribution of the high death rates. These figures show that the northern macroregion of Pianura Padana was the most affected area due to its higher economic activity and peculiar geographical conformation, i.e. a large plain surrounded by high mountains, where air tends to stagnate more than in other areas of the country. In general, the PM$_{2.5}$ map shows that a large part of the country has dark brown areas above the World Health Organization's threshold (10 μg/m^3).

3. Econometric model

To test the impact of particulate matter controlling for potential concurring factors, we estimate the following equation:

$$
\begin{aligned}
\text{Excess Deaths}_{tm} = &\beta_0 + \beta_1 \, \text{Pollution(MA)}_{tm} + \beta_2 \, t + \beta_3 \, t^2 + \beta_4 \, t^3 \\
&+ \beta_5 \, \text{Days\_Since\_Lockdown}_t + \beta_6 \, \text{Population}_m + \beta_7 \, \text{Density}_m + \beta_8 \, \text{Over65}_m \\
&+ \beta_9 \, \text{Income}_m + \beta_{10} \, \text{Employees}_m + \beta_{11} \, \text{Essential\_Employees}_m \\
&+ \beta_{12} \, \text{Temperature(MA)}_{tm} + \beta_{13} \, \text{Mobility}_{tp} + \Sigma_r \gamma_r \, \text{DRegion}_{rm} + u_{tm} \quad (1)
\end{aligned}
$$

where our dependent variable (*Excess Deaths$_{tm}$*) is the difference between total deaths in 2020 in municipality *m* on day *t* and the 2015–19 total average deaths in the corresponding municipality and day of the year. The main independent variable of interest is *Pollution(MA)*, calculated as a moving average from day *t* - 10 to day *t* of PM$_{10}$ or PM$_{2.5}$, measured in municipality *m* on day *t*.[5] We introduce linear, quadratic, and cubic time trends (*t*, *t^2*, *t^3*) starting with the disease outbreak, which

is conventionally fixed as February 24, 2020 (the beginning of our sample period) among control variables. These trends capture part of the deterministic evolution of the pandemic consistently with standard epidemiological modeling approaches (further robustness checks for heterogeneous pandemic dynamics are presented and discussed in section 6).[6] Among other controls, *Days_Since_Lockdown* counts the days since the national lockdown, taking into account the three government decisions that progressively introduced mobility restrictions in Italian municipalities.[7] *Population* is the number of residents in municipality *m* from the last Italian census (2011) (per 1000 inhabitants); *Density* is the population density in municipality *m* (per 1000 inhabitants); *Over65* is the proportion of people aged 65 or above and living in municipality *m* (per 1000 inhabitants); *Income* is the total before-tax income in municipality *m* (in billion euros); *Employees* and *Essential-Employees* are the number of employees operating in all sectors and in essential sectors only (per 1000 inhabitants) at the municipal level. The essential sectors are those on a list of activities that the Italian government allowed to operate during the lockdown.[8] These last two variables capture lockdown-induced local differences in job commuting flows due to the different incidences of essential and non-essential sectors in each municipality. *Temperature(MA)* is the 11-day (from t$_{-10}$ to t) moving average of daily air temperature in each municipality. Last, we control for time-varying human interactions with a variable (*Mobility*) measuring transit in the subways, bus and train stations, seaports, taxi stands, highway rest stops, and car rental agencies in Italian provinces. The variable is calculated in first differences, that is, as a change in the number of people in the above-mentioned transit areas compared to the baseline of the median value, for the corresponding day of the week, during the previous 5-week period. We also add region dummies (*DRegion*) to control for time-invariant features of the regions, such as urbanization rate or health system characteristics. In fact, health policies in Italy are run at the regional level, thereby making health capital endowments highly heterogeneous across regions.[9] Standard errors are clustered at the municipal level. A detailed description of variables and their sources is given in Table A1 in the Appendix.

Table 1 presents descriptive statistics of the variables used in our econometric specifications. As expected, the moving averages used in the estimates smooth extreme values of pollution and atmospheric indicators, with maxima of moving averages of particulate concentration reaching 45.71 and 61.72 μg/m^3, respectively. Nonetheless, the mean value of the PM$_{2.5}$ moving average (14.02 μg/m^3) during the sample period is above the average yearly threshold suggested by the

---

[5] The window length is as broadly consistent with the combined expected long- and short-term effects of PM as additional factors of contagion and diseases. As is well known, the mean incubation period of the virus is estimated between 4 and 6 days (Li et al., 2020). The interval between the onset of the illness and hospitalization in the most serious cases around 4 days (Docherty et al., 2020) and the decease outcome for the most unfortunate events about 9 days (Chen et al., 2020). With a sensitivity analysis we find that this window length provides the strongest effect in terms of magnitude.

[6] We perform Wald and Likelihood ratio test on nested hypotheses comparing the chosen specification with an alternative specification using only linear and quadratic terms. All tests confirm that the chosen specification is to be preferred. Our main findings are, however, robust also to this change (see the online Appendix). Findings of our robustness checks using day fixed effects are discussed in section 5.

[7] More specifically, based on the timeline of Italian government decision we have: i) Law Decree of 22 February establishing lockdown for eleven municipalities from 23th February to 8th March 2020 (Codogno, Castiglione d'Adda, Casalpusterlengo, Fombio, Maleo, Somaglia, Bertonico, Terranova dei Passerini, Castelgerundo e San Fiorano) and Vo Euganeo; ii) Law Decree on 7th March 2020 establishing lockdown for Lombardy and other 14 Center-North provinces (Modena, Parma, Piacenza, Reggio nell'Emilia, Rimini, Pesaro and Urbino, Alessandria, Asti, Novara, Verbano-Cusio-Ossola, Vercelli, Padova, Treviso, Venezia) since 8th March; iii) lockdown extended to all country since 10th March; iv) slowdown starting from 4th May to 14th June.

[8] The list of essential sectors has been created with DPCM (Decreto del Presidente del Consiglio dei Ministri) of 22nd March 2020 revised with DPCM 25th March 2020.

[9] For instance, Veneto has a stronger network of local doctors, while Lombardia has strategically aimed to concentrate care in large hospitals; furthermore, provinces in Lombardia have the lowest ratio of local doctors per inhabitant in Italy.
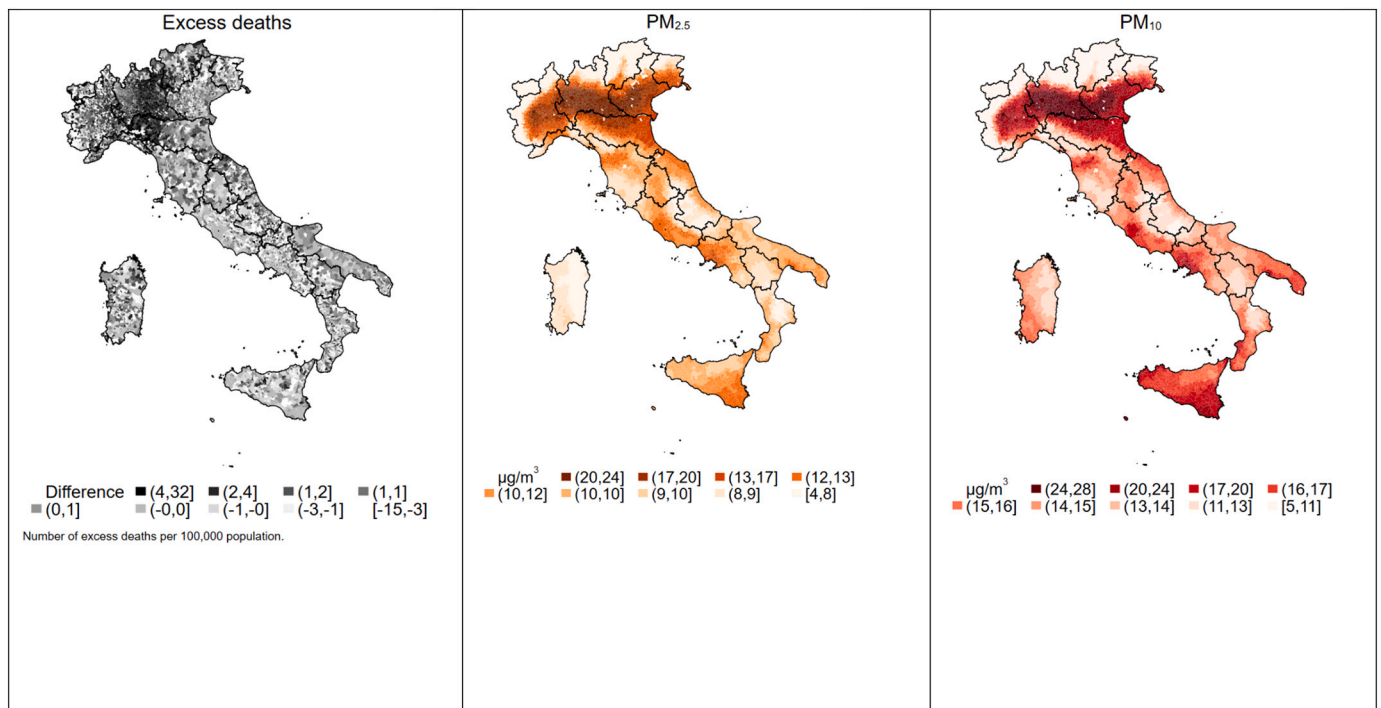
Fig. 1. A–C. Excess deaths, PM2.5 and PM10 in Italian municipalities.

Note: *Excess deaths* is the daily difference of total deaths in 2020 and the 2015–19 average total deaths at municipality level (Source: Istat); PM$_{2.5}$ is the 11-day (from t_{-10} to t) moving average of particulate matter with diameter < 2.5 μm (μg/m^3); PM$_{10}$ is the 11-day (from t_{-10} to t) moving average of particulate matter with diameter < 2.5 μm (μg/m^3).

Table 1
Descriptive statistics.

Variable	Obs	Mean	St. Dev.	Min	Max
Excess deaths	713244	0.011	0.252	−14.708	14.925
PM$_{2.5}$[*]	713244	14.022	7.408	1.862	45.714
PM$_{10}$[*]	713244	18.679	8.948	2.522	61.715
Rain[*]	713244	2.390	2.449	0.0002	18.331
Days since lockdown	713244	35.307	26.684	0	98
Population	713244	7.715	41.816	0.034	2617.175
Density	713244	0.307	0.659	0.001	12.924
Over 65	713244	1.79	10.70.	0.007	638.523
Income	713244	0.108649	0.783832	0.542792	49314.36
Employees	713244	2.248	17.862	0.001	1023.890
Employees in essential sectors	711480	0.985	9.607	0.001	547.307
Mobility	713244	−3.092	15.927	−79	65
Temperature (MA)[*]	713244	11.376	4.862	−11.15	24.47014

[*] Contains modified Copernicus Climate Change Service Information [2017–2020], DOI: 10.24381/cds.e2161bac'. Contains modified Copernicus Atmospheric Monitoring Service Information [2017–2020].

World Health Organization (10 μg/m^3).[10] Our sample period covered the end of winter and spring, and therefore we did not observe extreme hot temperature events (the single-day maximum is 28.86, while the moving average maximum 24.47).

4. Results

Before running our estimates, we perform panel stationarity tests and find that all our series are stationary. More specifically, we perform the

Lein-Lin-Chu (2020) test for unit roots in panel datasets and find that the null of non-stationarity is rejected in all cases (p < 0.001 for all series)[11].

In Table 2, we present the results of our main econometric specification. Columns 1 and 2 display (unweighted) pooled OLS estimates of the effects of PM$_{2.5}$ and PM$_{10}$, respectively. In columns 3 and 4, observations are weighted for the inverse of the distance from the centroid to give more importance to municipality centroids that lie closer to the geographical point of our meteorological observation of PM.

Our empirical findings show that the high mortality in 2020 is significantly and positively related to both air pollution measures. In terms of magnitude, the effect of PM$_{2.5}$ is larger than that of PM$_{10}$, with results from weighted and unweighted estimates for the same pollution variable being quite similar. The estimated pollution effect in column 3 implies that 1 μg/m^3 of additional PM$_{2.5}$ concentration creates an approximately 10% increase in the average value of the dependent variable, that is 0.113 extra deaths per day per 100,000 inhabitants, which corresponds to a 3.32% increase in mortality rate. The total effect over the 94 days of the pandemic considered in our sample is 1.07 extra excess deaths per 100,000 inhabitants. This implies that the effect over the entire Italian population is about 647.96 extra deaths per μg/m^3. Based on our coefficient magnitude, we estimate that a difference of about 19 μg/m^3 between the municipalities with the highest and lowest PM$_{2.5}$ average concentration in the sample would generate a difference of 1231.13 more deaths in the overall sample period.

The linear, quadratic, and cubic trends are strongly significant among the control variables and with the expected sign, displaying non-linear pandemic dynamics during the first phase. The share of employees in essential sectors is positive and significant and likely to capture the positive effect of high death rates on economic activity in industries that could not stop their operations during the lockdown. Time-varying

---

[10] https://www.who.int/news/item/02-05-2018-9-out-of-10-people-worldwide-breathe-polluted-air-but-more-countries-are-taking-action.

[11] Results available upon request.

Table 2
Pooled OLS estimates.

Variables	(1)	(2)	(3)	(4)
$PM_{2.5}$	0.000966***		0.00113***	
	(6.86e-05)		(9.95e-05)	
PM_{10}		0.000590***		0.000660***
		(3.74e-05)		(5.59e-05)
T (linear day trend)	0.00282***	0.00287***	0.00286***	0.00294***
	(0.000129)	(0.000129)	(0.000185)	(0.000186)
T^2 (quadratic day trend)	−7.88e-05***	−8.58e-05***	−8.10e-05***	−9.05e-05***
	(5.35e-06)	(5.14e-06)	(1.10e-05)	(1.12e-05)
T^3 (Cubic day trend)	4.80e-07***	5.11e-07***	4.87e-07***	5.30e-07***
	(3.11e-08)	(3.01e-08)	(5.84e-08)	(5.91e-08)
Days since lockdown	0.000686**	0.00100***	0.000830	0.00123*
	(0.000281)	(0.000272)	(0.000645)	(0.000652)
Population	−8.03e-05	−7.14e-05	−0.000135*	−0.000122*
	(5.58e-05)	(4.99e-05)	(7.27e-05)	(6.37e-05)
Density	−0.00274***	−0.00236***	−0.00300***	−0.00249***
	(0.000457)	(0.000429)	(0.000560)	(0.000527)
Over 65	0.000978***	0.000875***	0.00134***	0.00118***
	(0.000357)	(0.000313)	(0.000484)	(0.000418)
Income	−0.0136***	−0.0123***	−0.0180***	−0.0159***
	(0.00329)	(0.00298)	(0.00510)	(0.00456)
Employees	−0.000453**	−0.000382**	−0.000460	−0.000323
	(0.000206)	(0.000192)	(0.000311)	(0.000295)
Employees in Essential Sectors	0.00130***	0.00112***	0.00152**	0.00120**
	(0.000395)	(0.000367)	(0.000614)	(0.000578)
Temperature	−0.000333**	−0.000154	−0.000263	−1.02e-05
	(0.000162)	(0.000163)	(0.000337)	(0.000342)
Mobility	7.99e-05***	6.80e-05***	7.16e-05	5.84e-05
	(2.46e-05)	(2.45e-05)	(6.21e-05)	(6.20e-05)
Region dummies	Yes	Yes	Yes	Yes
Constant	−0.0218***	−0.0184***	−0.0223***	−0.0181***
	(0.00228)	(0.00214)	(0.00363)	(0.00349)
Observations	685,451	685,451	685,451	685,451
Log Likelihood	36,835	36,827	6369	6339

Note: Columns (1) and (2) do not weight observations, while columns (3) and (4) use as weight the inverse distance of municipality centroids from the meteorological point of observation. Standard errors clustered at municipality level in parentheses. Contains modified Copernicus Climate Change Service Information [2017–2020], DOI: 10.24381/cds.e2161bac. Contains modified Copernicus Atmospheric Monitoring Service Information [2017–2020]; *** p < 0.01, ** p < 0.05, * p < 0.1.

mobility is, as expected, positive and significant as an increase in people in transit stations has a positive and significant effect on excess deaths. The negative sign of the density variable can be explained by the fact that, with population among the regressors, the variable captures the positive effect of municipality surface on excess deaths, likely to be explained by how far inhabitants are from institutions and less accessible health services. The positive and significant effect on excess deaths of the share of the elder population at the municipal level is also expected.

We implement an instrumental variable approach from omitted variables and reverse causality to mitigate a possible estimation bias deriving from measurement error in the dependent variable (Table 3). We instrument the PM moving averages in Eq. (1) with the four-day lagged corresponding 11-day moving average of daily rainfalls controlling in our estimates for the mobility variable. We can confidently

Table 3
Pooled IV estimates.

Variables	(1)	(2)
$PM_{2.5}$	0.00117***	
	(0.000297)	
PM_{10}		0.000522***
		(0.000133)
T (linear day trend)	0.00303***	0.00329***
	(0.000227)	(0.000189)
T^2 (quadratic day trend)	−6.52e-05***	−8.14e-05***
	(1.01e-05)	(6.49e-06)
T^3 (Cubic day trend)	3.98e-07***	4.78e-07***
	(5.41e-08)	(3.68e-08)
Days since lockdown	−0.000155	0.000398
	(0.000386)	(0.000291)
Population	−8.73e-05***	−7.46e-05***
	(1.95e-05)	(1.89e-05)
Density	−0.00291***	−0.00227***
	(0.000392)	(0.000281)
Over 65	0.00104***	0.000878***
	(0.000121)	(0.000102)
Income	−0.0143***	−0.0121***
	(0.00149)	(0.00113)
Employees	−0.000497***	−0.000369***
	(0.000121)	(0.000105)
Employees in Essential Sectors	0.00140***	0.00110***
	(0.000246)	(0.000203)
Temperature	−0.000512*	−6.94e-05
	(0.000304)	(0.000213)
Mobility	1.01e-05	2.57e-05
	(2.79e-05)	(2.66e-05)
Region dummies	Yes	Yes
Constant	−0.0289***	−0.0244***
	(0.00317)	(0.00268)
Observations	670,865	670,865
Log Likelihood	35,659	35,648

Note: Contains modified Copernicus Climate Change Service Information [2017–2020], DOI: 10.24381/cds.e2161bac. Contains modified Copernicus Atmospheric Monitoring Service Information [2017–2020]; *** p < 0.01, ** p < 0.05, * p < 0.1.

argue that the chosen instrument is relevant since rainfalls have a strongly significant and negative effect on PM concentrations in the first-stage estimation.[12] The exclusion restriction is also likely to be satisfied in our case since—apart from its direct effects on pollution—it is implausible that four-day lagged rainfall moving averages significantly affect the difference in deaths between 2020 and the previous years on a given day. Rainfall may discourage mobility and reduce contagion or increase car vs. public-transport mobility (again reducing contagion), thereby potentially invalidating the exclusion restriction. However, these potential threats to the exclusion restriction can be excluded since we condition for mobility in all estimates. Furthermore, most of the mobility decisions made during the lockdown that cover most of our sample period were forced, with little impact on atmospheric conditions. The pairwise correlation between rain and mobility during lockdown is 0.03, which supports our hypothesis. This is a positive (yet low in magnitude) and non-statistically significant correlation, which goes against the prediction of a potential negative association between the two variables. Furthermore, the instrument is not statistically significant if we introduce it in our baseline non-instrumented specification (Eq. (1)), further supporting its validity hypothesis. Our main findings remain unchanged and the coefficient magnitude is remarkably close to the non-instrumented estimates.

In Table 4, we re-estimate our benchmark specification through OLS panel fixed effects. This allows for capturing unobservable time

---

[12] The null of weak identification is rejected with both Cragg-Donald Wald F statistic (58,131.46, *p-value* < 0.001) and Kleibergen-Paap Wald F statistic (76,201.84, *p-value* < 0.001) for the estimate in Table 3, Column 1. Findings are similar and the null hypothesis is rejected also for estimates in columns 2–4.

Table 4
OLS panel fixed-effects estimates.

Variables	(1)	(2)	(3)	(4)
$PM_{2.5}$	0.00123***		0.00145***	
	(7.60e-05)		(0.000144)	
PM_{10}		0.000644***		0.000713***
		(3.80e-05)		(5.87e-05)
T (linear day trend)	0.00295***	0.00298***	0.00302***	0.00307***
	(0.000131)	(0.000131)	(0.000195)	(0.000196)
T^2 (quadratic day trend)	−5.59e-05***	−7.10e-05***	−5.33e-05***	−7.35e-05***
	(5.52e-06)	(5.28e-06)	(8.85e-06)	(9.41e-06)
T^3 (Cubic day trend)	3.54e-07***	4.28e-07***	3.33e-07***	4.34e-07***
	(3.17e-08)	(3.07e-08)	(5.01e-08)	(5.13e-08)
Days Since Lockdown	−0.000670**	0.000134	−0.000794	0.000251
	(0.000303)	(0.000285)	(0.000505)	(0.000535)
Temperature	−0.000409*	−0.000404*	−0.000425	−0.000375
	(0.000219)	(0.000221)	(0.000419)	(0.000427)
Mobility	0.000107***	8.00e-05***	9.97e-05*	6.81e-05
	(2.49e-05)	(2.46e-05)	(5.70e-05)	(5.88e-05)
Constant	−0.0271***	−0.0207***	−0.0317***	−0.0234***
	(0.00247)	(0.00227)	(0.00592)	(0.00503)
Number of municipalities	7260	7260	7260	7260
Observations	685,451	685,451	685,451	685,451
Log Likelihood	41,862	41,837	11,200	11,146

Note: Columns (1) and (2) do not weight observations, while columns (3) and (4) use as weight the inverse distance of municipality centroids from the meteorological point of observation. Standard errors clustered at municipality level in parentheses. Contains modified Copernicus Climate Change Service Information [2017–2020], DOI: 10.24381/cds.e2161bac. Contains modified Copernicus Atmospheric Monitoring Service Information [2017–2020]; *** p < 0.01, ** p < 0.05, * p < 0.1.

Table 5
IV panel fixed-effect estimates.

Variables	(1)	(2)
$PM_{2.5}$	0.00158***	
	(0.000270)	
PM_{10}		0.000736***
		(0.000126)
T (linear day trend)	0.00380***	0.00385***
	(0.000194)	(0.000192)
T^2 (quadratic day trend)	−3.02e-05***	−5.36e-05***
	(1.06e-05)	(7.15e-06)
T^3 (Cubic day trend)	2.10e-07***	3.26e-07***
	(5.67e-08)	(4.01e-08)
Days since lockdown	−0.00282***	−0.00161***
	(0.000563)	(0.000409)
Temperature	−0.000800***	−0.000583**
	(0.000249)	(0.000233)
Mobility	4.84e-05*	4.80e-05*
	(2.63e-05)	(2.63e-05)
Constant	−0.0318	−0.0231
	(3.473e+10)	(3.473e+10)
Wald $\chi2$	1618.25	1618.07
Observations	670,865	670,865
Number of municipalities	7260	7260

Note: Contains modified Copernicus Climate Change Service Information [2017–2020], DOI: 10.24381/cds.e2161bac. Contains modified Copernicus Atmospheric Monitoring Service Information [2017–2020]; robust standard errors in parentheses. *** p < 0.01, ** p < 0.05, * p < 0.1.

invariant idiosyncratic factors at the finest geographical unit, e.g. the quality of local majors or local health governance at the municipality level. The significance of the $PM_{2.5}$ and PM_{10} variables is also confirmed in this model. In Table 5, we instrument the PM moving average as the fixed-effect estimates with the instrument used in Table 3. Our results are again confirmed.

5. Prolonged exposure vs. short term effects: decomposing the total PM effect

The 11-day moving average used so far mainly captures the time-varying effect of PM on excess deaths. However, it is reasonable to assume that this measure is also influenced by a long-term component capturing long-term, pre-COVID exposure to PM. This component is regarded as the crucial factor affecting the negative consequences of COVID-19 infection, according to the first strand of the literature described in the introduction.

To disentangle the effects deriving from these two—long-term structural and short-term time–varying—components, we propose the following decomposition. First, since the time-varying component can be correlated with historical levels of PM concentration, we regress the PM 11-day moving average, that is, *Pollution(MA),* on (time-invariant) average PM concentration in the two years before the pandemic, i.e., *PM (2018–2019)*. More specifically, we estimate the following model:

$$\text{Pollution(MA)}_{tm} = \beta_0 + \beta_1 \, \text{PM(2018–2019)}_m + \varepsilon_{tm} \tag{2}$$

Then, we compute the time-varying residuals $\widehat{\varepsilon}_{tm}$, which can be interpreted as a "cleaner" measure of the time-varying effect, i.e., the variation Pollution$(MA)_{tm}$ that is not explained by the variation in the long-term PM component.

We, therefore, run our benchmark model as in Eq. (1) by replacing *Pollution(MA)* with its time-varying residual component $\widehat{\varepsilon}_{tm}$, and the two-year (time-invariant) average of PM concentration. The estimating model reads as:

$$\begin{aligned}\text{Excess Deaths}_{tm} = {} & \beta_0 + \beta_1 \, \widehat{\varepsilon}_{tm} + \beta_2 \, \text{PM(2017–2018)}_m + \beta_3 \, t + \beta_4 \, t^2 + \beta_5 \, t^3 \\ & + \beta_6 \, \text{Days\_Since\_Lockdown}_t + \beta_7 \, \text{Population}_m + \beta_8 \, \text{Density}_m + \beta_9 \, \text{Over65}_m \\ & + \beta_{10} \, \text{Income}_m + \beta_{11} \, \text{Employees}_m + \beta_{12} \, \text{Essential\_Employees}_m \\ & + \beta_{13} \, \text{Temperature(MA)}_{tm} + \beta_{14} \, \text{Mobility}_{tp} + \Sigma_r \gamma_r \, \text{DRegion}_{rm} + u_{tm}\end{aligned} \tag{3}$$

The results from the OLS pooled estimates of Eq. (3) show that the coefficients of both components (β_1 and β_2) are positive and statistically significant (columns 1 and 2 of Tables 6 −7 for $PM_{2.5}$ and PM_{10}, respectively). Our interpretation is that long-term exposure and time-varying effect significantly predict excess mortality.

We also re-estimate Eq. (3) through an OLS fixed-effects model. The results are in columns 3 and 4 of Tables 6–7 for $PM_{2.5}$ and PM_{10}, respectively. Given the nature of this regression model, the effect of pre-COVID time-invariant exposure to PM is now absorbed by municipality fixed effects. The rationale of this last estimate is to check whether the time-varying PM component is statistically significant when local unobserved time-invariant characteristics are accounted for. Our findings confirm that this is the case.

6. Robustness checks

The first robustness check we perform features the use of an alternative instrument calculated as the residual from the following regression:

$$\text{Pollution(MA)}_{tm} = \gamma_0 + \gamma_1 \, \text{Mobility}_{tp} + \gamma_2 \, \text{Excess Deaths}_{tm} \, t + \gamma_3 \, \text{Rain(MA)} + \eta_{tm} \tag{4}$$

The residual η_{tm} is, by construction, exogenous when used as an instrument in our benchmark estimate in Eq. (1). The advantage of this instrument is that through Eq. (4), we control for the complex pattern of relationships through which rain and mobility can affect the relationship between pollution and excess deaths.

The new IV findings confirm that this instrument is also relevant since first-stage regression coefficients are significant. Moreover, the falsification exercise of introducing the instrument in non-instrumented estimates confirms that the former has no significant direct impact on the dependent variable. In terms of magnitude, we note, however, that the coefficient size of the instrumented variable is much higher in the

Table 6
Decomposition of the long-term and short-term effects.

Variables	(1)	(2)	(3)	(4)
$PM_{2.5}$ (short term component)	0.000850***	0.000872***	0.00110***	0.00119***
	(6.79e-05)	(9.71e-05)	(7.65e-05)	(0.000114)
$PM_{2.5}$ (ex-ante component)	0.000945***	0.00127***		
	(0.000177)	(0.000264)		
T (linear day trend)	0.00312***	0.00327***	0.00347***	0.00368***
	(0.000157)	(0.000226)	(0.000162)	(0.000237)
T^2 (quadratic day trend)	-7.67e-05***	−8.34e-05***	−5.21e-05***	−5.56e-05***
	(4.95e-06)	(1.11e-05)	(5.30e-06)	(8.95e-06)
T^3 (cubic day trend)	4.60e-07***	4.91e-07***	3.27e-07***	3.42e-07***
	(2.82e-08)	(5.71e-08)	(2.98e-08)	(4.85e-08)
Population	−8.02e-05	−0.000135*		
	(5.33e-05)	(7.12e-05)		
Employees	−0.000434**	−0.000430		
	(0.000200)	(0.000307)		
Density	−0.00252***	−0.00285***		
	(0.000451)	(0.000550)		
Employees in Essential sectors	0.00124***	0.00144**		
	(0.000383)	(0.000605)		
Income	−0.0129***	−0.0174***		
	(0.00319)	(0.00507)		
Over 65	0.000944***	0.00131***		
	(0.000341)	(0.000475)		
Days since lockdown	0.000318	0.000598	−0.00135***	−0.00131**
	(0.000290)	(0.000709)	(0.000324)	(0.000571)
Temperature	−0.000252	−0.000304	−0.000515**	−0.000492
	(0.000182)	(0.000368)	(0.000219)	(0.000407)
Mobility	3.96e-05	2.86e-05	6.27e-05**	5.33e-05
	(2.49e-05)	(6.56e-05)	(2.50e-05)	(6.28e-05)
Constant	−0.0251***	−0.0275***	−0.0172***	−0.0132***
	(0.00291)	(0.00469)	(0.00251)	(0.00473)
Municipality fixed effects	No	No	Yes	Yes
Observations	685,385	685,385	685,385	685,385
Log Likelihood	37,948	7547	42,993	12,422
Number of Municipalities			7260	7260

Columns (1) and (2) pooled estimates, columns (3) and (4) fixed effect estimates. Standard errors clustered at municipality level in parentheses. Contains modified Copernicus Climate Change Service Information [2017–2020], DOI: 10.24381/cds.e2161bac. Contains modified Copernicus Atmospheric Monitoring Service Information [2017–2020]; *** $p < 0.01$, ** $p < 0.05$, * $p < 0.1$.

new IV estimates than in the non-IV ones.

We also test whether the short-term effect estimated in our decomposition exercise presented in Tables 6 and 7 remains significant when instrumented under our two different IV approaches. We find this to be the case (Panel 8.5, columns 1 and 2).

There are two additional potential concerns in our estimates: (i) heterogeneity of the pandemic dynamics at the municipal level; and (ii) spatial dependence of the pandemic.

With regard to the first concern, we take two approaches. First, we estimate the Pesaran and Smith (1995) mean group estimator model where slope coefficients are separately calculated for each municipality and averaged across all municipalities. Our main variables of interest remain strongly significant. However, this approach corrects more for heterogeneity of PM impact than of the virus spread net of the PM effect. We, therefore, estimate this model with a mean group estimator specification allowing for province-specific trends. Again, our main results are unchanged (Table 8, panel 8.5, column 4). Second, we test whether our findings are confirmed when data are aggregated at the province level as the problem of heterogeneous infection dynamics is particularly severe at the municipal level, but less so at the province level. Our main findings are confirmed in non-instrumented and instrumented specifications with province-level data (Table 9). Finally, we check for the contemporaneous presence of PM between and within effects to test whether particulate matter has an impact through both effects at the municipal level. This is another way to address the heterogeneity of pandemic dynamics problem since PM between-effects cannot be affected by such a problem. To this purpose, we estimate hybrid models that split the effect of particulate matter into within- and between-municipality effects (Schunck, 2013; Schunck and Perales, 2017) using a Mundlak (1978) random-effects approach. The estimated findings

show that both between and a within municipality variation in $PM_{2.5}$ and PM_{10} significantly matter in explaining variation in excess deaths. The within-effect, however, has more power since it accounts for three-fourth of the overall effect in the decomposition estimated in the hybrid model (Table 8, panel 8.5, column 3). Note that this decomposition allows us to disentangle contemporary between and within effects; this is a different approach from that proposed in section 4 Eq. (3), where the between effect is long term, lagged, and aims to capture previous long-term exposure to particulate matter.

For the second concern, that is, spatial correlation, we run a spatial Durbin model for our panel with the province level data following the approach proposed by Belotti et al. (2017).

Furthermore, to account for other possible endogeneity issues, we build a spatial panel IV model. First, we run the fixed-effects quasi-maximum likelihood estimator on the endogenous regressor against both the instruments and the exogenous covariates of the main model. Then, after getting the control function, ie., the prediction of the overall error component from this regression, we run the full spatial model again, controlling for this component. This allows us to further mitigate the remaining endogeneity of the PM variables (Table 9, panel 9.5, columns 1–3).

To check whether our findings are robust to a more flexible control for the aggregate pandemic dynamics that do not assume any particular functional form, we repeat our estimates by introducing day fixed effects (Table 8, panels 8.1–8.4). Our main results remain significant and the coefficient magnitude do not vary significantly.

In an additional robustness check, we calculate COVID-19 non-synchronous regional trends by assuming independent regional pandemic dynamics. To this purpose, we set the regional contagions at n = 100 and use this conventional number as the starting point of the pandemic

Table 7
Decomposition of the long-term and short term effects.

	(1)	(2)	(3)	(4)
PM_{10} (short term component)	0.000494***	0.000489***	0.000563***	0.000577***
	(3.60e-05)	(5.24e-05)	(3.79e-05)	(5.28e-05)
PM_{10} (ex-ante component)	0.000666***	0.000955***		
	(0.000149)	(0.000226)		
T (linear day trend)	0.00313***	0.00329***	0.00342***	0.00363***
	(0.000158)	(0.000230)	(0.000161)	(0.000236)
T^2 (quadratic day trend)	−8.24e-05***	−8.95e-05***	−6.60e-05***	−7.22e-05***
	(4.80e-06)	(1.07e-05)	(5.00e-06)	(9.19e-06)
T^3 (cubic day trend)	4.84e-07***	5.18e-07***	3.94e-07***	4.23e-07***
	(2.76e-08)	(5.53e-08)	(2.85e-08)	(4.89e-08)
Population	−7.63e-05	−0.000132**		
	(5.01e-05)	(6.68e-05)		
Employees	−0.000394**	−0.000361		
	(0.000193)	(0.000303)		
Density	−0.00233***	−0.00266***		
	(0.000438)	(0.000550)		
Employees in Essential sectors	0.00114***	0.00129**		
	(0.000368)	(0.000597)		
Income	−0.0122***	−0.0165***		
	(0.00303)	(0.00486)		
Over 65	0.000892***	0.00125***		
	(0.000317)	(0.000443)		
Days since lockdown	0.000630**	0.000925	−0.000532*	−0.000364
	(0.000280)	(0.000692)	(0.000304)	(0.000582)
Temperature	−0.000225	−0.000293	−0.000423*	−0.000354
	(0.000187)	(0.000361)	(0.000220)	(0.000414)
Mobility	3.53e-05	2.51e-05	5.26e-05**	4.41e-05
	(2.49e-05)	(6.58e-05)	(2.50e-05)	(6.30e-05)
Constant	−0.0220***	−0.0247***	−0.0155***	−0.0132***
	(0.00285)	(0.00450)	(0.00250)	(0.00473)
Municipality fixed effects	No	No	Yes	Yes
Observations	685,385	685,385	685,385	685,385
Log Likelihood	37,941	7532	42,969	12,384
Number of Municipalities			7260	7260

Columns (1) and (2) pooled estimates, columns (3) and (4) fixed effect estimates. Standard errors clustered at municipality level in parentheses. Contains modified Copernicus Climate Change Service Information [2017–2020], DOI: 10.24381/cds.e2161bac. Contains modified Copernicus Atmospheric Monitoring Service Information [2017–2020]; *** $p < 0.01$, ** $p < 0.05$, * $p < 0.1$.

trends in each region. This approach allows us to account for unobserved time-varying region-level characteristics. Our main findings do not change after attributing a specific regional trend to each municipal (Table 10, panels 3–5,8–10, 13 and 16).[13]

We further refine our main instrument by ruling out episodes of extreme rainfalls from the sample. More specifically, we eliminate observations where the instrument (rainfall moving average) is above the 95th centile and can be suspected to directly affect excess deaths (Table 10, panels 2,4-5,7,9–10, 12 and 15).

To test whether our findings are robust for "super-spreader" events during the pandemic, we consider the UEFA Champions League match between Atalanta and Valencia that took place February 19, 2020, when around 40,000 Atalanta supporters gathered in the San Siro stadium in Milan for the match.[14] To do so, we repeat our estimates by removing data for the Bergamo and Milano provinces. Again, the results remain unchanged in terms of magnitude (the pooled estimate coefficient changes only at the fifth decimal digit) and statistical significance (Table 10, panels 1,4-5,6,9–10, 11 and 14).

7. Discussion

To compare the magnitude of our results with those of the existing literature, we calculate what our coefficients imply in terms of the impact of 1 μg/m^3 of PM on mortality. For the magnitude of the PM

effects, the estimated PM coefficients vary between different estimates that look at different sources of variability. However, presenting all of them at least as a robustness check is important to evaluate the robustness and extension of the significance of our findings. For example, the fixed-effect coefficient compared with its pooled estimated counterpart captures only the within-effect controlling for unobserved time-invariant municipality effects. The IV effect depends in turn on the quality of the instrument and corrects for endogeneity problems.

Based on all our different estimates, we conclude that the overall non-instrumented $PM_{2.5}$ effect can be reasonably estimated in a range between 0.001 and 0.002. The highest coefficient is that of the fixed effect estimates augmented for day fixed effects. The same numbers for the PM_{10} effect are between 0.0006 and 0.001, also when considering estimates of provincial data in Table 8 and robustness checks in Table 9. Given the average daily mortality rate in Italy in the last four years, the effect implies that one additional μg/m^3 of $PM_{2.5}$ is associated with an increase in mortality rate by 2.9 to 5.59%. This effect is in the range of findings made in other studies, slightly above that estimated in the Netherland (Cole et al., 2020) and below that obtained in the US (Wu et al., 2020) and Northern Italy (Cocker et al. 2020) (see introduction).

Note that the severe lockdown measures adopted at the beginning of March 2020 significantly contributed to air quality. The lockdown, therefore, reduced the short term effect of PM on high mortality rate during the pandemic. To understand to what extent this occurred, we calculated the difference between the average daily PM concentration during the pandemic's first wave (February 2020 to May 2020) and during the corresponding days in the previous two years (2018–2019

---

[13] Table 10 presents a summary of the empirical findings from these final robustness checks. Full findings are in the online Appendix.
[14] https://www.wsj.com/articles/the-soccer-match-that-kicked-off-italys-cor onavirus-disaster-11585752012.

Table 8
Robustness checks: day effects and alternative specifications.

Panel 8.1	(1)	(2)	(3)	(4)	(5)	(6)
	Pooled OLS	Pooled IV	Pooled IV (second instrument*)	OLS panel fixed effects	IV panel fixed effects	IV panel fixed effects (second instrument*)
Day effects						
$PM_{2.5}$	0.00141***	0.00174***	0.00284***	0.00178***	0.00203***	0.00692***
	(8.20e-05)	(0.000281)	(0.000478)	(9.39e-05)	(0.000238)	(0.000911)
PM_{10}	0.000907***	0.000645***	0.00182***	0.00101***	0.000824***	0.00271***
	(4.60e-05)	(0.000104)	(0.000290)	(4.84e-05)	(9.72e-05)	(0.000367)
Panel 8.2						
Day effects (with inverse distance weights)						
$PM_{2.5}$	0.00158***			0.00201***		
	(0.000123)			(0.000185)		
PM_{10}	0.00101***			0.00111***		
	(7.40e-05)			(9.20e-05)		

Panel 8.3	(1)	(2)	(3)	(4)
	Pooled OLS decompositition	OLS panel fixed effects decomposition	IV panel fixed effects decomposition	IV panel fixed effects decomposition (second instrument*)
Day effects				
$PM_{2.5}$ (short term component)	0.00148***	0.00173***	0.00202***	0.00678***
	(8.48e-05)	(9.42e-05)	(0.000242)	(0.000911)
PM_{10} (short term component)	0.000847***	0.000956***	0.00212***	0.00775***
	(4.41e-05)	(4.76e-05)	(0.000252)	(0.00106)
$PM_{2.5}$ (ex ante component)	0.00118***			
	(0.000187)			
PM_{10} (ex ante component)	0.00101***			
	(0.000162)			
Panel 8.4				
Day effects (with inverse distance weights)				
$PM_{2.5}$ (short term component)	0.00156***	0.00191***		
	(0.000122)	(0.000175)		
PM_{10} (short term component)	0.000885***	0.00102***		
	(6.36e-05)	(8.26e-05)		
$PM_{2.5}$ (ex ante component)	0.00150***			
	(0.000270)			
PM_{10} (ex ante component)	0.00130***			
	(0.000234)			

Panel 8.5	(1)	(2)	(3)	(4)	(5)	(6)
	IV panel fixed effects decomposition	IV panel fixed effects decomposition (second instrument*)	Hybrid model	Pesaran model	Pooled IV (second instrument)	IV panel fixed effects (second instrument*)
Other specifications						
$PM_{2.5}$				0.0006873***	0.00300***	0.00537***
				(0.0001148)	(0.000472)	(0.000727)
PM_{10}				0.0004479***	0.00235***	0.00383***
				(0.0000771)	(0.000370)	(0.000518)
$PM_{2.5}$ (Between Effect)			0.000481***			
			(0.000174)			
PM_{10} (Between Effect)			0.000429**			
			(0.000167)			
$PM_{2.5}$ (Within Effect)			0.00123***			
			(7.32e-05)			
PM_{10} (Within Effect)			0.000644***			
			(4.20e-05)			
$PM_{2.5}$ (short term component)	0.00113***	0.00583***				
	(0.000247)	(0.000712)				
PM_{10} (short term component)	0.00134***	0.00602***				
	(0.000293)	(0.000736)				

Table 8 (*continued*)

Panel 8.5	(1)	(2)	(3)	(4)	(5)	(6)
	IV panel fixed effects decomposition	IV panel fixed effects decomposition (second instrument*)	Hybrid model	Pesaran model	Pooled IV (second instrument)	IV panel fixed effects (second instrument*)
$PM_{2.5}$ (ex ante component)						
PM_{10} (ex ante component)						

Second instrument: instrument built as explained in Eq. (4) section 5. Robust standard errors in parentheses. *** $p < 0.01$, ** $p < 0.05$, * $p < 0.1$.

Table 9
Provincial specifications and robustness checks: day effects and other specifications.

Panel 9.1	(1)	(2)	(4)	(5)
	Pooled OLS	Pooled IV	OLS panel fixed effects	IV panel fixed effects
$PM_{2.5}$	0.00113***	0.00123***	0.000783***	0.00131***
	(0.000189)	(6.73e-05)	(0.000108)	(6.39e-05)
PM_{10}	0.000766***	0.000936***	0.000516***	0.000991***
	(0.000127)	(5.30e-05)	(6.85e-05)	(4.94e-05)

Panel 9.2	(1)	(2)	(4)	(5)
	Pooled OLS	Pooled IV	OLS panel fixed effects	IV panel fixed effects
Day effects				
$PM_{2.5}$	0.000740***	0.00198***	0.000800***	0.00146***
	(0.000163)	(0.000155)	(0.000146)	(0.000104)
PM_{10}	0.000475***	0.000752***	0.000407***	0.000684***
	(1.00e-04)	(5.88e-05)	(7.12e-05)	(4.89e-05)

Panel 9.3	(7)	(8)	(9)
	Pooled OLS decompositition	OLS panel fixed effects decomposition	IV panel fixed effects decomposition
$PM_{2.5}$ (short term component)	0.000765***	0.000783***	0.00131***
	(0.000125)	(4.82e-05)	(6.39e-05)
PM_{10} (short term component)	0.000584***	0.000516***	0.000991***
	(8.02e-05)	(2.33e-05)	(4.94e-05)
$PM_{2.5}$ (ex ante component)	0.00196***		
	(0.000403)		
PM_{10} (ex ante component)	0.00159***		
	(0.000397)		

Panel 9.4	(7)	(8)	(9)
	Pooled OLS decompositition	OLS panel fixed effects decomposition	IV panel fixed effects decomposition
Day effects			
$PM_{2.5}$ (short term component)	0.000733***	0.000800***	0.00146***
	(0.000161)	(5.27e-05)	(0.000104)
PM_{10} (short term component)	0.000404***	0.000407***	0.000684***
	(7.25e-05)	(2.48e-05)	(4.89e-05)
$PM_{2.5}$ (ex ante component)	0.000953***		
	(0.000334)		
PM_{10} (ex ante component)	0.000876**		
	(0.000375)		

Panel 9.5	(1)					(2)					(3)
	Spatial panel fixed effects with time dependence					Spatial IV panel fixed effects with time dependence					Pesaran Model
Other specifications											
	Main	Wx	Direct	Indirect	Total	Main	Wx	Direct	Indirect	Total	
$PM_{2.5}$	0.00976	0.00369**	0.0146**	0.0653***	0.0798***	0.0217**	0.00334**	0.0277***	0.0810***	0.109***	0.000661***
	(0.00668)	(0.00147)	(0.00602)	(0.00967)	(0.00844)	(0.00897)	(0.00148)	(0.00879)	(0.0120)	(0.0163)	(1.00e-04)
PM_{10}	0.00897**	0.00203**	0.0121***	0.0419***	0.0540***	0.0161***	0.00182*	0.0199***	0.0513***	0.0712***	0.000350***
	(0.00408)	(0.000948)	(0.00363)	(0.00637)	(0.00525)	(0.00565)	(0.000955)	(0.00551)	(0.00778)	(0.0103)	(5.22e-05)

Table 10
Robustness checks.

Panel 10.1 Pooled estimates excluding super-spreader events	(1)	(2)	(3)	(4)
PM$_{10}$		0.000561***		0.000619***
		(3.89e-05)		(5.54e-05)
PM$_{2.5}$	0.000972***		0.00113***	
	(7.24e-05)		(0.000101)	
Observations	650,491	650,491	650,491	650,491
Log Likelihood	43,826	43,812	10,945	10,911

Standard errors clustered at municipality level in parentheses
*** p < 0.01, ** p < 0.05, * p < 0.1

Panel 10.2 Pooled estimates excluding extreme rainfalls	(1)	(2)	(3)	(4)
PM$_{10}$		0.000592***		0.000659***
		(3.97e-05)		(5.84e-05)
PM$_{2.5}$	0.00102***		0.00119***	
	(7.67e-05)		(0.000111)	
Observations	632,772	632,772	632,772	632,772
Log Likelihood	30,652	30,639	274.6	240.9

Standard errors clustered at municipality level in parentheses
*** p < 0.01, ** p < 0.05, * p < 0.1

Panel 10.3 Pooled estimates using nonsynchronous regional epidemic trends	(1)	(2)	(3)	(4)
PM$_{10}$		0.000826***		0.000907***
		(3.86e-05)		(6.20e-05)
PM$_{2.5}$	0.00136***		0.00152***	
	(6.76e-05)		(0.000108)	
Observations	685,451	685,451	685,451	685,451
Log Likelihood	36,645	36,615	6175	6119

Standard errors clustered at municipality level in parentheses
*** p < 0.01, ** p < 0.05, * p < 0.1

Panel 10.4 Instrumental variable estimates	Excluding super-spreader events		Excluding extreme rainfalls		Using nonsynchronous regional epidemic trends	
	(1)	(2)	(3)	(4)	(5)	(6)
PM$_{10}$		0.000554***		0.000698***		0.000411***
		(0.000134)		(0.000153)		(0.000132)
PM$_{2.5}$	0.00156***		0.00144***		0.00114***	
	(0.000378)		(0.000317)		(0.000365)	
Observations	622,993	622,993	632,772	632,772	656,481	656,481
Log Likelihood	38,810	38,797	30,632	30,636	31,428	31,309

Robust standard errors in parentheses
*** p < 0.01, ** p < 0.05, * p < 0.1.

Panel 10.5 Instrumental variable estimates (using second instrument)	Excluding super-spreader events		Excluding extreme rainfalls		Using nonsynchronous regional epidemic trends	
	(1)	(2)	(3)	(4)	(5)	(6)
PM$_{10}$		0.00215***		0.00256***		0.00369***
		(0.000690)		(0.000378)		(0.000194)
PM$_{2.5}$	0.00343***		0.00326***		0.00514***	
	(0.00110)		(0.000481)		(0.000270)	
Observations	626,590	626,590	644,381	644,381	682,408	682,408
Log Likelihood	39,767	39,661	34,319	33,712	35,885	34,972

Second instrument: instrument built as explained in Eq. (4) section 5. Robust standard errors in parentheses
*** p < 0.01, ** p < 0.05, * p < 0.1

Panel 10.6 Fixed effect estimates excluding super-spreader events	(1)	(2)	(3)	(4)
PM$_{10}$		0.000589***		0.000659***
		(3.96e-05)		(6.13e-05)
PM$_{2.5}$	0.00118***		0.00143***	
	(8.11e-05)		(0.000159)	
Observations	650,491	650,491	650,491	650,491
Log Likelihood	48,363	48,338	15,317	15,261

Standard errors clustered at municipality level in parentheses
*** p < 0.01, ** p < 0.05, * p < 0.1

Panel 10.7 Fixed effect estimates excluding extreme rainfalls	(1)	(2)	(3)	(4)
PM$_{10}$		0.000652***		0.000716***
		(4.08e-05)		(6.53e-05)

Table 10 (*continued*)

Panel 10.7 Fixed effect estimates excluding extreme rainfalls	(1)	(2)	(3)	(4)
PM_{25}	0.00133***		0.00155***	
	(8.72e-05)		(0.000172)	
Observations	632,772	632,772	632,772	632,772
Log likelihood	35,963	35,931	5370	5310

Standard errors clustered at municipality level in parentheses
*** $p < 0.01$, ** $p < 0.05$, * $p < 0.1$

Panel 10.8 Fixed effect estimates using nonsynchronous regional epidemic trends	(1)	(2)	(3)	(4)
PM_{10}		0.000844***		0.000918***
		(4.02e-05)		(6.96e-05)
$PM_{2.5}$	0.00156***		0.00174***	
	(7.58e-05)		(0.000152)	
Observations	685,451	685,451	685,451	685,451
Log Likelihood	41,799	41,744	11,128	11,040

Standard errors clustered at municipality level in parentheses
*** $p < 0.01$, ** $p < 0.05$, * $p < 0.1$

Panel 10.9 Fixed effect instrumental variable estimates	Excluding super-spreader events		Excluding extreme rainfalls		Using nonsynchronous regional epidemic trends	
	(1)	(2)	(3)	(4)	(5)	(6)
PM_{10}		0.00113***		0.00105***		0.000713***
		(0.000140)		(0.000145)		(0.000114)
$PM_{2.5}$	0.00223***		0.00199***		0.00166***	
	(0.000274)		(0.000274)		(0.000264)	
Observations	643,646	643,646	632,772	632,772	656,481	656,481
Log Likelihood	2436.33	2436.13	3484.09	3483.71	1773.10	1772.53

Robust standard errors in parentheses
*** $p < 0.01$, ** $p < 0.05$, * $p < 0.1$

Panel 10.10 Fixed effect instrumental variable estimates (using second instrument)	Excluding super-spreader events		Excluding extreme rainfalls		Using nonsynchronous regional epidemic trends	
	(1)	(2)	(3)	(4)	(5)	(6)
PM_{10}		0.00138***		0.00407***		0.00390***
		(0.000499)		(0.000518)		(0.000200)
$PM_{2.5}$	0.00190***		0.00564***		0.00565***	
	(0.000688)		(0.000716)		(0.000289)	
Observations	647,448	647,448	644,381	644,381	682,408	682,408
Log Likelihood	2381.78	2380.58	3465.80	3435.37	2204.38	2196.61

Second instrument: instrument built as explained in Eq. (4) section 5. Robust standard errors in parentheses
*** $p < 0.01$, ** $p < 0.05$, * $p < 0.1$

Panel 10.11 Decomposition between fixed and time varying $PM_{2.5}$ effects: exclusion of super spreader events				
Dep. Var.: diffsupop1819	(1)	(2)	(3)	(4)
$PM_{2.5}$ (short term component)	0.000815***	0.000835***	0.00113***	0.00123***
	(7.17e-05)	(9.93e-05)	(8.18e-05)	(0.000124)
$PM_{2.5}$ (ex ante component)	0.00148***	0.00163***		
	(0.000183)	(0.000258)		
Observations	650,425	650,425	650,425	650,425
Log likelihood	44,962	12,242	49,517	16,652

Standard errors clustered at municipality level in parentheses
*** $p < 0.01$, ** $p < 0.05$, * $p < 0.1$

Panel 10.12 Decomposition between fixed and time varying $PM_{2.5}$ effects: exclusion of extreme rainfalls	(1)	(2)	(3)	(4)
$PM_{2.5}$ (short term component)	0.000795***	0.000819***	0.00105***	0.00114***
	(6.91e-05)	(9.81e-05)	(7.85e-05)	(0.000118)
$PM_{2.5}$ (ex ante component)	0.000909***	0.00126***		
	(0.000184)	(0.000279)		
Observations	647,135	647,135	647,135	647,135
Log Likelihood	34,708	3761	39,973	8806

Standard errors clustered at municipality level in parentheses
*** $p < 0.01$, ** $p < 0.05$, * $p < 0.1$

Panel 10.13 Decomposition between fixed and time varying $PM_{2.5}$ effects: nonsynchronous regional epidemic trends	(1)	(2)	(3)	(4)
$PM_{2.5}$ (short term component)	0.00124***	0.00128***	0.00147***	0.00156***
	(6.89e-05)	(9.57e-05)	(7.57e-05)	(0.000127)
$PM_{2.5}$ (ex ante component)	0.00152***	0.00187***		

Table 10 (*continued*)

Panel 10.13 Decomposition between fixed and time varying $PM_{2.5}$ effects: nonsynchronous regional epidemic trends	(1)	(2)	(3)	(4)
	(0.000173)	(0.000271)		
Observations	685,385	685,385	685,385	685,385
Log Likelihood	37,745	7329	42,921	12,340
Standard errors clustered at municipality level in parentheses				
*** p < 0.01, ** p < 0.05, * p < 0.1				

Panel 10.14 Decomposition between fixed and time varying PM_{10} effects: exclusion of super spreader events	(1)	(2)	(3)	(4)
PM_{10} (short term component)	0.000756***	0.000840***	0.000996***	0.00114***
	(6.58e-05)	(9.17e-05)	(7.25e-05)	(0.000127)
PM_{10} (ex ante component)	0.00119***	0.00134***		
	(0.000152)	(0.000199)		
Observations	664,139	664,139	664,139	664,139
Log Likelihood	47,740	14,379	52,244	18,705
Standard errors clustered at municipality level in parentheses				
*** p < 0.01, ** p < 0.05, * p < 0.1				

Panel 10.15 Decomposition between fixed and time varying PM_{10} effects: exclusion of extreme rainfalls	(1)	(2)	(3)	(4)
PM_{10} (short term component)	0.000863***	0.000920***	0.00111***	0.00122***
	(6.80e-05)	(8.95e-05)	(7.65e-05)	(0.000132)
PM_{10} (ex ante component)	0.000792***	0.00113***		
	(0.000158)	(0.000243)		
Observations	647,135	647,135	647,135	647,135
	34,724	3782	39,993	8833
Standard errors clustered at municipality level in parentheses				
*** p < 0.01, ** p < 0.05, * p < 0.1				

Panel 10.16 Decomposition between fixed and time varying PM_{10} effects: nonsynchronous regional epidemic trends	(1)	(2)	(3)	(4)
PM_{10} (short term component)	0.00115***	0.00122***	0.00132***	0.00143***
	(6.31e-05)	(9.38e-05)	(6.79e-05)	(0.000126)
PM_{10} (ex ante component)	0.00121***	0.00149***		
	(0.000145)	(0.000207)		
Observations	699,835	699,835	699,835	699,835
Log Likelihood	40,745	9723	45,874	14,644
Standard errors clustered at municipality level in parentheses				
*** p < 0.01, ** p < 0.05, * p < 0.1				

The table reports synthetic statistics for PM coefficients in three different robustness checks. In the first panel we remove provinces of Milan and Bergamo to account for the super-spreader event of the Champions League match Atalanta-Valencia. In the second panel we exclude from the sample observations where moving average rainfalls are above 95th centile. In the third panel we replace the national (linear, quadratic, cubic) trend variables measuring contagion dynamics with nonsynchronous regional trend variables starting from the day of the 100th contagion in the given region. For tables 10.1 to 10.3 and 10.6–10.8, columns (1) and (2) do not weight observations, while columns (3) and (4) use as weight the inverse distance of municipality centroids from the meteorological point of observation. For tables 10.11 to 10.16, columns (1) and (2) presents pooled estimates, while columns (3) and (4) fixed effect estimates.

average). If we limit our analysis to the Northern regions,[15] the difference is above 1 µg. Hence, if we can interpret estimates in section 4 as causal, we may conclude that lockdown measures saved between 1 and 2 extra deaths per 100,000 inhabitants.

Extracting the PM concentration differential using fixed-effects estimates do not change the significance and magnitude, thereby confirming our previous analysis.

This study has a number of caveats and limitations. First, our instruments are relevant, but we cannot test their validity and have to prove that on logical grounds. However, the instruments' lack of significance when included as explanatory variables in the main specification, the control for time-varying mobility, the robustness in the sensitivity analysis when excluding extreme rainfalls supports our exclusion restriction.

Second, data at the municipal level are rarely available and, when available, come from the last census in 2011. Consequently, while our analysis controls for many variables like the share of population aged above 65 and the number of employees, we cannot control for other possible factors influencing COVID-19 contagion. For instance, we cannot control for the number of doctors in a given municipality.

However, this characteristic is likely captured by municipality fixed effects at the finest level of geographical disaggregation. In our robustness checks described in section 5, we account for municipal heterogeneous pandemic dynamics looking at between effects, using province trends in mean group estimators, and aggregating data at the province level. Note that the two above-mentioned and all other unobserved components were invariant during our 3-month sample period but updated in time to the 2011 census. Third, similarly to other papers (see Cocker et al. 2020), our dependent variable measures total deaths and does not discriminate between COVID-19 deaths and deaths caused by other diseases. This is because of the heterogeneity of COVID-19-related deaths registration, both over time and across regions, that we have explained when motivating the choice of our dependent variable.

A final consideration relates to the interpretation of our findings on the decomposition between the two-year average and the time-varying component of PM. The first fixed component captures the ex-ante long-term exposure effect, while the second the effect of changes in PM during the pandemic. We do not explicitly and exclusively identify this last component in the "short term effect." Therefore, it can be questioned whether the time-varying effect derives from the PM capacity to increase survival outside the human body (short term effect) or it may further weaken the capacity of lungs and alveoli to resist respiratory and pulmonary diseases on top of the long-term exposure. While further research could clarify this point, this paper is the first, to the best

---

[15] Valle d'Aosta, Piemonte, Lombardia, Trentino-Alto-Adige, Friuli-Venezia-Giulia, Liguria, Emilia-Romagna, Marche, Toscana.

of our knowledge, to show that historical pre-COVID and contemporary time-varying effects matter.

8. Conclusions

Two research hypotheses in the literature on the impact of particulate matter on COVID-19 contagion and deaths argue that prolonged *pre-COVID* exposure to, and *contemporary* levels of particulate matter can play a positive and significant role.

To test these two hypotheses, we evaluate the impact of particulate matter concentration in Italian municipalities on daily deaths between the first COVID-19 outbreak in Italy and the previous five years. The specific contribution of this study to the literature hinges on the use of the geographically finest controls for concurring factors through municipality fixed-effects, instrumental variable estimates to tackle endogeneity issues within a model taking spatial correlation into account, and the decomposition of the two effects, that is, long-term pre-COVID exposure and time-varying effect.

Our findings show that the impact of both components is positive and significant. Our estimates control for standard time-trend components accounting for the non-linear deterministic evolution of the pandemic, the effects of lockdown measures, and several other controls, such as time-varying mobility. Additional results from province-level data accounting for spatial correlation and instrumental variable estimates addressing endogeneity problems further underline the robustness of our findings. More specifically, taking an average $PM_{2.5}$ effect estimated across all our different models, we find that particulate matter concentration predicts more than 1231 more deaths if we consider the difference between the municipalities with the highest and lowest average $PM_{2.5}$ concentration during the first pandemic wave.

Indeed, our instrumental-variable estimates are inevitably subject to discussion and limitations. However, if they can be interpreted as causal, our empirical results have relevant policy implications. They highlight an additional and important reason to contrast particulate matter beyond those already known. For example, beyond the impact of atmospheric phenomena, the sources of PM depend on around 90% of human choices such as domestic heating systems, mobility, agriculture, and industrial production processes. Therefore, urgent steps should be taken to accelerate the transition to frontier technology, reducing each source's contribution to PM.

Declaration of Competing Interest

The authors declare that they have no known competing financial interests or personal relationships that could have appeared to influence the work reported in this paper.

Appendix A. Appendix

Table A1
Variable legend.

Variable	Description	Source
PM_{10}	11-day (from t_{-10} to t) moving average of particulate matter with diameter < 10 μm ($μg/m^3$)	Copernicus Atmospheric Monitoring Service (CAMS) -
$PM_{2.5}$	11-day (from t_{-10} to t) moving average of particulate matter with diameter < 2.5 μm ($μg/m^3$)	Copernicus Atmospheric Monitoring Service (CAMS) -
Excess Deaths	Daily difference of total deaths in 2020 and the 2015–19 average total deaths at municipality level	Italian National Statistical Institute
Mobility	Number of people in transit in subway, bus, train stations, sea port, taxi stand, highway rest stop and car rental agencies in the given Italian province (Change compared to the baseline of the median value, for the corresponding day of the week, during the previous 5-week period).	Google: Community Mobility Report
Population	Number of residents in 2011 at municipality level per 1000 inhabitants.	Italian National Statistical Institute
Employees	Number of employees operating in all economic sectors at municipality level per 1000 inhabitants.	Italian National Statistical Institute
Employees in Essential Sectors	Number of employees operating in essential economic sectors (as defined by the Decree of the Italian President of the Municipality of Ministers, released on March 22nd and revised on March 25th), at municipality level per 1000 inhabitants.	Italian National Statistical Institute
Density	Population per municipality area per 1000 inhabitants.	Italian National Statistical Institute
Over 65	Share of people aged 65 or above per 1000 inhabitants.	Italian National Statistical Institute
Income	Total municipality gross income (billion euros)	Italian National Statistical Institute
Rain	11-day (from t_{-10} to t) moving average of total precipitation in mm at municipality level	Copernicus Climate Change Service (CCCS)
Temperature	11-day (from t_{-10} to t) moving average of air temperature measure at the height of 2 m above ground, at municipality level.	Copernicus Climate Change Service (CCCS)
Region	Italian regions.	
Days since lockdown	Days since the start of the national lockdown considering the different starting days based on subsequent government decisions (see footnote 7).	

Appendix B. Supplementary data

Supplementary data to this article can be found online at https://doi.org/10.1016/j.ecolecon.2022.107340.

References

Anderson, M.L., 2020. As the wind blows: the effects of long-term exposure to air pollution on mortality. J. Eur. Econ. Assoc. 18 (4), 1886–1927.

Austin, Wes, et al., 2020. COVID-19 Mortality and Contemporaneous Air Pollution. No. paper2016. International Center for Public Policy, Andrew Young School of Policy Studies, Georgia State University.

Becchetti, L., Beccari, G., De Santis, D., 2020. Lagged Particulate Matter, Contagions and Deaths: The Relationship between Quality of Air and COVID-19 at European Level. Cefims dp 159.

Becchetti, L., Conzo, G., Conzo, P., Salustri, F., 2022. Understanding the heterogeneity of COVID-19 deaths and contagions: The role of air pollution and lockdown decisions. Journal of Environmental Management 305, 114316. https://doi.org/10.1016/j.jenvman.2021.114316.

Belotti, F., Hughes, G., Piano Mortari, A., 2017. Spatial panel-data models using Stata. Stata J. 17 (1), 139–180.

Bontempi, E., 2020. First data analysis about possible COVID-19 virus airborne diffusion due to air particulate matter (PM): the case of Lombardy (Italy). Environ. Res. 109639.

Cakmak, S., Hebbern, C., Pinault, L., Lavigne, E., Vanos, J., Crouse, D.L., Tjepkema, M., 2018. Associations between long-term PM2. 5 and ozone exposure and mortality in

the Canadian census health and environment cohort (CANCHEC), by spatial synoptic classification zone. Environ. Int. 111, 200–211.

Cartenì, A., Di Francesco, L., Martino, M., 2020. How mobility habits influenced the spread of the COVID-19 pandemic: results from the Italian case study. Sci. Total Environ. 741, 140489.

Chen, J., Qi, T., Liu, L., Ling, Y., Qian, Z., Li, T., Li, F., Xu, Q., Zhang, Y., Xu, S., Song, Z., Zeng, Y., Shen, Y., Shi, Y., Zhu, T., Lu, H., 2020. Clinical progression of patients with covid-19 in shanghai, China. J. Inf. Secur. 80 (5), e1–e6.

Ciencewicki, J., Jaspers, I., 2007. Air pollution and respiratory viral infection. Inhal. Toxicol. 19 (14), 1135–1146.

Coker, E.S., Cavalli, L., Fabrizi, E., Guastella, G., Lippo, E., Parisi, M.L., Vergalli, S., 2020. The effects of air pollution on COVID-19 related mortality in northern Italy. Environ. Resour. Econ. 76 (4), 611–634.

Cole, M., Ozgen, C., Strobl, E., 2020. Air Pollution Exposure and COVID-19.

Comunian, S., Dongo, D., Milani, C., Palestini, P., 2020. Air pollution and Covid-19: the role of particulate matter in the spread and increase of Covid-19's morbidity and mortality. Int. J. Environ. Res. Public Health 17 (12), 4487.

Delnevo, G., Mirri, S., Roccetti, M., 2020. Particulate matter and COVID-19 disease diffusion in Emilia-Romagna (Italy). Already a cold case? Computation 8 (2), 59.

Docherty, A.B., Harrison, E.M., Green, C.A., Hardwick, H.E., Pius, R., Norman, L., Holden, K.A., Read, J.M., Dondelinger, F., Carson, G., Merson, L., Lee, J., Plotkin, D., Sigfrid, L., Halpin, S., Jackson, C., Gamble, C., Horby, P.W., Nguyen-Van-Tam, J.S., Ho, A., Russell, C.D., Dunning, J., Openshaw, P.J., Baillie, J.K., Semple, M.G., 2020. Features of 20 133 UK patients in hospital with covid-19 using the isaric who clinical characterisation protocol: prospective observational cohort study. BMJ 369.

Faustini, A., Stafoggia, M., Berti, G., Bisanti, L., Chiusolo, M., Cernigliaro, A., Vigotti, M. A., 2011. The relationship between ambient particulate matter and respiratory mortality: a multi-city study in Italy. Eur. Respir. J. 38 (3), 538–547.

Isphording, I.E., Pestel, N., 2020. Pandemic Meets Pollution: Poor Air Quality Increases Deaths by COVID-19.

Jeong, S.C., Cho, Y., Song, M.K., Lee, E., Ryu, J.C., 2017. Epidermal growth factor receptor (EGFR)—MAPK—nuclear factor (NF)-κB—IL8: a possible mechanism of particulate matter (PM) 2.5-induced lung toxicity. Environ. Toxicol. 32 (5), 1628–1636.

Kim, K.H., Kabir, E., Kabir, S., 2015. A review on the human health impact of airborne particulate matter. Environ. Int. 74, 136–143.

Li, Q., Guan, X., Wu, P., Wang, X., Zhou, L., Tong, Y., Ren, R., Leung, K.S., Lau, E.H., Wong, J.Y., Xing, X., Xiang, N., Wu, Y., Li, C., Chen, Q., Li, D., Liu, T., Zhao, J., Liu, M., Tu, W., Chen, C., Jin, L., Yang, R., Wang, Q., Zhou, S., Wang, R., Liu, H., Luo, Y., Liu, Y., Shao, G., Li, H., Tao, Z., Yang, Y., Deng, Z., Liu, B., Ma, Z., Zhang, Y., Shi, G., Lam, T.T., Wu, J.T., Gao, G.F., Cowling, B.J., Yang, B., Leung, G.M., Feng, Z., 2020. Early transmission dynamics in Wuhan, China, of novel coronavirus infected pneumonia. N. Engl. J. Med. 382 (13), 1199–1207 (PMID: 31995857).

Magazzino, C., Mele, M., Schneider, N., 2020. The relationship between air pollution and COVID-19-related deaths: an application to three French cities. Appl. Energy 115835.

McGuinn, L.A., Ward-Caviness, C., Neas, L.M., Schneider, A., Di, Q., Chudnovsky, A., Kraus, W.E., 2017. Fine particulate matter and cardiovascular disease: comparison of assessment methods for long-term exposure. Environ. Res. 159, 16–23.

Mundlak, Y., 1978. On the pooling of time series and cross section data. Econometrica 46, 69–85.

Ogen, Y., 2020. Assessing nitrogen dioxide (NO2) levels as a contributing factor to the coronavirus (COVID-19) fatality rate. Sci. Total Environ. 138605.

Pelucchi, C., Negri, E., Gallus, S., Boffetta, P., Tramacere, I., La Vecchia, C., 2009. Long-term particulate matter exposure and mortality: a review of European epidemiological studies. BMC Public Health 9 (1), 453.

Perone, G., 2020. The determinants of COVID-19 case fatality rate (CFR) in the Italian regions and provinces: an analysis of environmental, demographic, and healthcare factors. Sci. Total Environ. 142523.

Pesaran, M. Hashem, Smith, Ron P., 1995. Estimating long-run relationships from dynamic heterogeneous panels. J. Econ. 68 (1), 79–113.

Pinault, L.L., Weichenthal, S., Crouse, D.L., Brauer, M., Erickson, A., van Donkelaar, A., Brook, J.R., 2017. Associations between fine particulate matter and mortality in the 2001 Canadian census health and environment cohort. Environ. Res. 159, 406–415.

Schunck, R., 2013. Within and between estimates in random-effects models: advantages and drawbacks of correlated random effects and hybrid models. Stata J. 13, 65–76.

Schunck, R., Perales, F., 2017. Within- and between-cluster effects in generalized linear mixed models: a discussion of approaches and the xthybrid command. Stata J. 17, 89–115.

Sedlmaier, N., Hoppenheidt, K., Krist, H., Lehmann, S., Lang, H., Büttner, M., 2009. Generation of avian influenza virus (AIV) contaminated fecal fine particulate matter (PM2. 5): genome and infectivity detection and calculation of immission. Vet. Microbiol. 139 (1–2), 156–164.

Setti, L., Passarini, F., De Gennaro, G., Di Gilio, A., Palmisani, J., Buono, P., Rizzo, E., 2020. Position Paper Relazione circa l'effetto dell'inquinamento da particolato atmosferico e la diffusione di virus nella popolazione. SIMA-Società Italiana di Medicina Ambientale.

Travaglio, M., Yu, Y., Popovic, R., Leal, N.S., Martins, L.M., 2021. Links between air pollution and COVID-19 in England. Environmental Pollution 268 (Part A), 115859. https://doi.org/10.1016/j.envpol.2020.115859.

Wu, X., Nethery, R.C., Sabath, B.M., Braun, D., Dominici, F., 2020. Air pollution and COVID-19 mortality in the United States: Strengths and limitations of an ecological regression analysis. Science Advances 6 (45). https://doi.org/10.1126/sciadv.abd4049.

Yin, P., Brauer, M., Cohen, A., Burnett, R.T., Liu, J., Liu, Y., Zhou, M., 2017. Long-term fine particulate matter exposure and nonaccidental and cause-specific mortality in a large national cohort of Chinese men. Environ. Health Perspect. 125 (11), 117002.

Yongjian, Z., Jingu, X., Fengming, H., Liqing, C., 2020. Association between short-term exposure to air pollution and COVID-19 infection: evidence from China. Sci. Total Environ. 138704.

Zoran, M.A., Savastru, R.S., Savastru, D.M., Tautan, M.N., 2020. Assessing the relationship between surface levels of PM2. 5 and PM10 particulate matter impact on COVID-19 in Milan, Italy. Sci. Total Environ. 738, 139825.